

Identification of subtype-specific genomic alterations in aggressive adult T-cell leukemia/lymphoma

Aya Oshiro, Hiroyuki Tagawa, Koichi Ohshima, Kennosuke Karube, Naokuni Uike, Yukie Tashiro, Atae Utsunomiya, Masato Masuda, Nobuyuki Takasu, Shigeo Nakamura, Yasuo Morishima, and Masao Seto

Aggressive adult T-cell leukemia/lymphoma (ATLL) such as acute and lymphoma types are fatal diseases with poor prognosis. Although these 2 subtypes feature different clinicopathologic characteristics, no detailed comparative analyses of genomic/genetic alterations have been reported. We performed array-based comparative genomic hybridization for 17 acute and 49 lymphoma cases as well as real-time quantitative polymerase chain reaction (PCR) to identify the target genes

of recurrently amplified regions. Comparison of the genome profiles of acute and lymphoma types revealed that the lymphoma type had significantly more frequent gains at 1q, 2p, 4q, 7p, and 7q, and losses of 10p, 13q, 16q, and 18p, whereas the acute type showed a gain of 3/3p. Of the recurrent high-level amplifications found at 1p36, 6p25, 7p22, 7q, and 14q32 in the lymphoma type, we were able to demonstrate that *CARMA1* is a possible target gene of the 7p22 amplification for

the lymphoma type but not for the acute type. Furthermore, we found *BCL11B* overexpression in the acute type regardless of the 14q32 gain/amplification, but no or low expression of the gene in the lymphoma type. These results suggest that acute and lymphoma types are genomically distinct subtypes, and thus may develop tumors via distinct genetic pathways. (Blood. 2006;107:4500-4507)

© 2006 by The American Society of Hematology

Introduction

Adult T-cell leukemia/lymphoma (ATLL) is a human T-lymphotropic virus type-I (HTLV-1)-mediated neoplasm.¹⁻³ ATLL develops tumors during a 40- to 70-year latency period from the time of HTLV-1 infection.⁴ The results of statistical analysis suggest that additional genetic alterations are essential for viral integrated T cells to become malignant.⁵

Four major clinical subtypes—smoldering, chronic, acute, and lymphoma—have been identified.⁶ The smoldering and chronic subtypes are characterized by an indolent clinical course, whereas the acute and lymphoma subtypes are aggressive and show poor prognosis, although their clinicopathologic features are clearly different. The acute type generally presents with hepatosplenomegaly, constitutional symptoms, elevated lactate dehydrogenase (LDH), and hypercalcemia,⁷ but these are seen less often in the lymphoma type. The lymphoma type is characterized by prominent lymphadenopathy without peripheral blood involvement, while the acute type is characterized by abnormal lymphocytes in peripheral blood and blood circulating in the whole body.⁷ These differences suggest that these 2 subgroups develop tumors via distinct genetic pathways.

Two cytogenetic and 1 comparative genomic hybridization (CGH) study of genomic aberrations of ATLL have been reported.⁸⁻¹⁰ The first 2 studies found that chromosome abnormalities of ATLL are complicated and occur more frequently in aggressive than in indolent ATLL. The third study, using conventional CGH analysis, showed that aggressive ATLL displayed more genomic gains and losses than the indolent type. However, despite these different clinicopathologic features of acute and lymphoma types, no comparative studies of the genomic aberrations of these subtypes have been reported. However, a comparative analysis of the genomic imbalances of these subtypes may provide important insights into the pathogenesis of aggressive ATLL.

To investigate the genomic aberrations of these subtypes, we performed high-resolution genome-wide array-based CGH (array CGH) for 17 patients with acute ATLL and 49 patients with lymphoma ATLL. For a further investigation of the relationship between genomic amplification and expression, we also performed quantitative real-time reverse transcription-polymerase chain reaction (RQ-PCR) to determine the target genes in some of the recurrent regions with high copy number gains.

From the Division of Molecular Medicine and Division of Hematology and Cell Therapy, Aichi Cancer Center Institute, Nagoya, Aichi; Department of Pathology, Kurume University School of Medicine, Kurume, Fukuoka; Department of Hematology, National Kyushu Cancer Center, Fukuoka; Department of Pathology, Imakiire General Hospital, Kagoshima; Department of Hematology, Imamura Bun-in Hospital, Kagoshima; Second Department of Internal Medicine, University Hospital, University of the Ryukyus, Nishihara, Okinawa; and Pathology/Clinical Laboratories, Nagoya University Hospital, Nagoya, Aichi, Japan.

Submitted September 22, 2005; accepted January 10, 2006. Prepublished online as *Blood* First Edition Paper, February 16, 2006; DOI 10.1182/blood-2005-09-3801.

Supported in part by a Grant-in-Aid from the Ministry of Health, Labor and Welfare; a Grant-in-Aid from the Ministry of Education, Culture, Sports, Science, and Technology; a Grant-in-Aid B2 and C from the Japan Society for

the Promotion of Science; a Grant-in-Aid from the Foundation of Promotion of Cancer Research; a Grant-in-Aid for Cancer Research from the Princess Takamatsu Cancer Research Fund (03-23503); and a Grant-in-Aid from the China Japan Medical Association. The Wella Award from the Japan Leukemia Research Fund was awarded to M.S.

The online version of this article contains a data supplement.

Reprints: Masao Seto, 1-1 Kanokoden, Chikusa-ku Nagoya, 464-8681, Japan; e-mail: mseto@aichi-cc.jp.

The publication costs of this article were defrayed in part by page charge payment. Therefore, and solely to indicate this fact, this article is hereby marked "advertisement" in accordance with 18 U.S.C. section 1734.

© 2006 by The American Society of Hematology

Patients, materials, and methods

ATLL patients

Samples of peripheral blood and lymph nodes, together with clinical data, were obtained from 66 patients under a protocol approved by the Institutional Review Board of the Aichi Cancer Center. Informed consent was provided according to the Declaration of Helsinki. The patients were selected from those hospitalized between 1992 and 2004 at Fukuoka University School of Medicine, the University of the Ryukyus School of Medicine, Imamura-Bunin Hospital, and their affiliated hospitals. We identified 17 patients with acute ATLL and 49 patients with lymphoma type ATLL. The median survival from the time of diagnosis was 5.9 months for acute type and 12.5 months for lymphoma type. The diagnosis of ATLL was based on clinical features, hematologic characteristics, immunophenotype, the presence of serum antibodies to ATLL-associated antigens, and monoclonal integration of HTLV-I proviral DNA. The immunophenotype of the tumors was determined by immunohistochemistry for tissue sections and/or flow cytometry for cell suspensions (CD2, CD3, CD5, CD7, CD4, CD8, CD25, and CD45RO). Monoclonal integration of HTLV-I proviral DNA into ATLL cells was assayed by means of Southern blotting analysis. For the clinical subtypes of ATLL the classification by Shimoyama et al of acute, lymphoma, chronic, and smoldering types was adopted.⁶

Acute type. The acute type is characterized by a leukemic phase with a markedly elevated white blood cell count that consists of mainly abnormal lymphocytes known as “flower cells.” The acute type is also characterized by hypercalcemia and/or a high LDH value (more than twice the upper limit of the normal range). Tumor specimens from all 17 patients, comprising 9 men and 8 women, were all obtained from the peripheral blood, which contained more than 60% leukemic cells (more than $10 \times 10^9/L$ [$10\,000/\mu L$]) at the time of diagnosis. The median age of the patients was 57 years (range, 44-78 years); 16 patients had elevated LDH, 9 had elevated serum calcium levels, and 9 had a poor performance status (Table 1).

Lymphoma type. The lymphoma type is characterized by prominent lymphadenopathy without peripheral blood involvement. Tumor specimens were obtained from 26 men and 23 women whose median age was 64 years old (range, 36-85 years). No leukemic cells were recognized in the peripheral blood at the time of diagnosis (Table 1).

Table 1. Characteristics of ATLL patients and their clinical features based on diagnostic criteria (n = 66)

Characteristic	Acute type	Lymphoma type
No. of patients	17	49
Median age, y (range)	57 (44-78)	64 (36-85)
Sex, no. male (%)	9 (53)	26 (53)
Performance status, no. (%)		
0-2	8 (47)	ND
Greater than 2	9 (53)	ND
Nodal involvement, no. (%)	7 (41)	49 (100)
Hepatosplenomegaly, no. (%)	6 (35)	ND
Cell type*	Peripheral blood	Lymph node
Flower cells†	+	-
Elevated WBC count‡, no. (%)	17 (100)	ND
LDH level, no. (%)		
Normal	1 (6)	ND
Elevated	16 (94)	ND
Ca level, no. (%)		
Normal	8 (47)	ND
Elevated	9 (53)	ND

ND indicates not determined; +, present; -, absent.

*Cell types from which the DNA was extracted: peripheral blood for acute type and lymph node for lymphoma type.

†Flower cells were observed in peripheral blood in all patients with acute-type ATLL, and in none of the patients with lymphoma-type ATLL.

‡Elevated WBC count defined as more than $10 \times 10^9/L$ ($10\,000/\mu L$).

DNA and RNA samples

High molecular weight DNA was extracted from lymph nodes and peripheral blood by using standard proteinase K/RNase treatment and phenol-chloroform extraction. DNA and RNA samples were extracted from frozen tissue. Normal DNA was obtained from the blood of healthy male donors. RNA was prepared from lymph nodes and peripheral blood by homogenization in guanidinium thiocyanate and centrifugation through cesium chloride.

Southern blotting for the HTLV-1 genome

Monoclonal integration of HTLV-I proviral DNA into ATLL cells was demonstrated by Southern blotting analysis. Briefly, high-molecular-weight DNA was extracted from mononuclear cells (MNCs). DNA samples (5 μg) were digested with *EcoRI* and size-fractionated on 0.75% agarose gels. They were then electrotransferred onto a nitrocellulose membrane and hybridized to randomly primed ³²P-labeled DNA probes specific for HTLV-I. Thereafter, the blots were washed at appropriate stringency and visualized by autoradiography.¹¹

Array-based CGH

The array consisted of 2304 BAC and PAC clones, covering the human genome at a resolution of roughly 1.3 Mb, from libraries RP11 and RP13 for BAC clones, and RP1, RP3, RP4 and RP5 for PAC clones. BAC and PAC clones were selected from the information from the National Center for Biotechnology Information (NCBI; <http://www.ncbi.nlm.nih.gov/>), Ensembl Genome Data Resources (<http://www.ensembl.org/>), and the University of California at Santa Cruz (UCSC) genome Bioinformatics, and obtained from the BACPAC Resource Center at the Children's Hospital (Oakland Research Institute, Oakland, CA). Clones were ordered from chromosomes 1 to 22 and X within each chromosome on the basis of Ensembl Genome Data Resources from the Sanger Center Institute (February 2005 version). The locations of all the clones used for array CGH were confirmed by fluorescence in situ hybridization (FISH). For the array, 10 simultaneous hybridizations of healthy male versus healthy male were performed to define the normal variation for the log₂ ratio. A total of 113 clones with less than 10% of the mean fluorescence intensity of all the clones, with the most extreme average test-over-reference ratio deviations from 1.0 and with the largest standard deviation in this set of normal controls excluded from further analyses.

A total of 2235 clones (covering 2988 Mb, 1.3 Mb of resolution) were therefore subjected to further analysis. Since more than 96% of the measured fluorescence log₂ ratio values at each spot (2 × 2235 clones) ranged from +0.2 to -0.2, the thresholds for the log₂ ratio of gains and losses were set at log₂ ratios of +0.2 and -0.2, respectively. Regions of low-level gain/amplification were defined as log₂ ratio +0.2 to +1.0; those suspected of containing a heterozygous loss/deletion were defined as log₂ ratio -1.0 to -0.2, and those showing high-level gain/amplification as log₂ ratio greater than +1.0, and those suspected of containing a homozygous losses/deletion as log₂ ratio less than -1.0.¹²⁻¹⁴

Real-time quantitative polymerase chain reaction

Expression levels of mRNA were measured by means of real-time fluorescence detection using a previously described method.¹⁵ Briefly, the primers of *CARMA1* were sense: 5'-CATTCTACATACCAAGGGGC-3' and antisense: 5'-ATCTGCTGCTGCAGCTTGAT-3'; the primers of *BCL11b* were sense: 5'-CAAGCAGGAGAACATTGCAG-3' and antisense: 5'-AGTGATCACGGATGAGTGAG-3'; the primers of *IRF4* were sense: 5'-AGAAGAGCATCTTCCGCATC-3' and antisense: 5'-TGCTCTGT-TCAAAGCGCAC-3'. The real-time PCR using SYBR Green I (Takara Bio, Tokyo, Japan) and the primers was performed with a Smart Cycler System (Takara Bio) according to the manufacturer's protocol. *G6PDH* served as an endogenous control, while the expression levels of *CARMA1* mRNA in each sample were normalized on the basis of the corresponding *G6PDH* content and recorded as relative expression levels. All the experiments were performed in duplicate.

Statistical analysis

To analyze genomic regions for statistical differences between the 2 patient groups, the data set was constructed as follows. Genomic alterations were defined by a \log_2 ratio threshold of +0.2 for copy number gain, and of -0.2 for copy number loss. Gained clones (\log_2 ratio > +0.2) were inputted as "1" versus no-gained clones (\log_2 ratio < +0.2) as "0" in an Excel template for each case (Microsoft, Redmond, WA). Similarly, lost clones (\log_2 ratio < -0.2) were inputted as "1" versus no-lost clones (\log_2 ratio > -0.2) as "0" in another Excel template. Cases showing genomic gain or loss were counted with an Excel template for each single clone (2235 clones in all) in the acute or the lymphoma group. Data analyses were then performed for the comparison of frequencies of gain or loss for each single clone between the acute and lymphoma groups (2235 tests each for gain and loss, 4470 tests in all). Fisher exact test for probability was used for the former analysis. The *P* value for screening of candidate clones was less than .05 for every analysis. When a candidate clone was identified, the clone's continuity with the subsequent clones was evaluated. In cases where the *n*th clone and subsequent *k* clones (*k* ≥ 0) were found to be candidate clones, the *P* value for continual association was calculated as $\prod_{i=n}^{n+k} p_i$ under the assumption that each clone is independent throughout the entire genome. As we applied multiple tests (4470 tests maximum), the conventional Bonferroni procedure was applied to define the alpha-error for the final conclusion.¹⁶ Therefore, we defined a $\prod_{i=n}^{n+k} p_i$ value of less than 0.05 per 4470 ($= 1 \times 10^{-5}$) as statistically significant.

The Mann-Whitney *U* test was used for detecting significant differences in expression levels of *IRF4* (6p25), *CARMA1* (7p22), and *BCL11B* (14q32) in groups with and without the genomic amplifications. All the statistical analyses were conducted with the STATA version 8 statistical package (StataCorp, College Station, TX).

Results

Detection of genomic imbalances in ATLL

Representative individual examples of the high-resolution analysis of 2 patient samples are shown in Figure S1 (see the Supplemental Figure link at the top of the online article, at the *Blood* website). Array CGH detected both small and large chromosome areas of gains and deletions as well as clear amplification and deletion borders. Gains and losses of genetic material obtained from 66 patients (49 with lymphoma ATLL and 17 with acute ATLL) were subjected to data analysis.

Genomic imbalances in acute type. Of the 17 patients analyzed, 1 sample did not show any copy number change. The entire tumor set, including the case without any genomic alterations characteristic of the acute type, involved average copy number gains of 221 Mb and 4.2 regions, and average copy number losses of 133 Mb and 4.5 regions (Table 2). Regions of recurrent (> 20%) gain were detected on chromosomes 3, 8p11.21-8q13.1, 8q24.21-24.23, 9p24.3-24.1, 9q33.3-34.3, 14q31.1-32.33, and X, and regions of recurrent loss on chromosomes 2q37.1-37.3, 4q21.1-24,

Table 2. Copy number alterations of ATLL

	Acute type	Lymphoma type
Copy number gain*		
Average genome size, Mb	221.5	356.46
Average % of the genome	7.5	12.2
Average no. of regions	4.18	9.69
Copy number loss*		
Average genome size, Mb	133.0	274.3
Average % of the genome	4.5	9.3
Average no. of regions	4.5	9.75

For acute-type ATLL, *n* = 17; for lymphoma-type ATLL, *n* = 49.

*Copy number change of X chromosome was excluded.

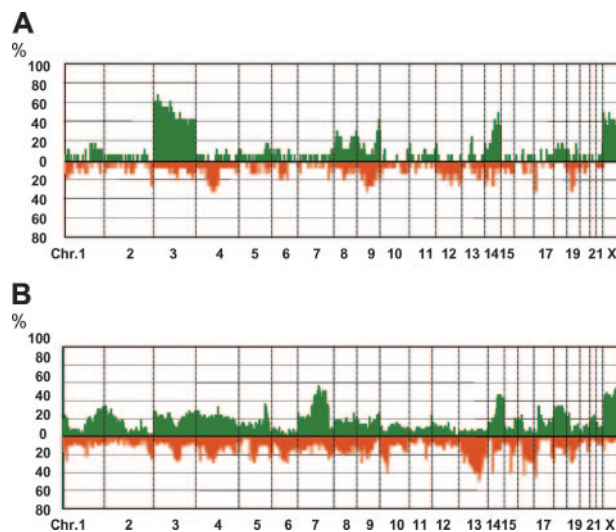


Figure 1. Genome-wide frequency of genomic imbalance in acute and lymphoma type ATLL. Horizontal lines indicate 2235 BAC/PAC clones listed in order from chromosomes 1 to 22 and X. Within each chromosome, clones are shown in order from the p to the q telomere in accordance with information from the Ensembl Genome Data Resources of the Sanger Center Institute (February 2005 version). Vertical lines indicate frequency (%) of gains and losses. (A) Acute type (17 patients). (B) Lymphoma type (49 patients). The green area represents genomic gain; red region, genomic loss.

6q14.1, 9q21.12-31.2, 17p13.1, and 19q13.31-13.2 (Figures 1A,2A).

Genomic imbalances in lymphoma type. Gains and losses of genetic materials obtained from 49 patient samples of the lymphoma type were subjected to data analysis. All of the cases demonstrated genomic aberrations. The entire tumor set involved average copy number gains of 356 Mb and 9.7 regions and average copy number losses of 274 Mb and 9.8 regions (Table 2). Regions of recurrent (> 20%) gain were detected on chromosomes 1p36.23-36.21, 1p21.3-23.3, 1p25.2-1q44, 2p25.1-22.3, 2p2.1-21, 3p26.3-q12.3, 3q25.2-29, 4p16.3-q12, 4q13-34.1, 6p25.3-24.1, 7p22.3-15.2, 7p14.3-14.2, 7p13-q36.3, 8q21.3-22.2, 8q24.22-24.21, 9p24.2-24.1, 9q34.3, 14q31.1-32.33, 18cen-23q, 21q21-22.2, and X, and losses at 1p31.2-12, 2q36.1-37.3, 3q13.13-24, 4q13.2-22.3, 5q15-23.1, 6q14.1-22.31, 8p23.3-21.2, 8q21.13, 9p21.3, 9q21.12-21.33, 10p15.3-cen., 13q12.3-34, 14q11.2-21.1, 16cen-16q24.1, 17p13.3-12, 18p11.32-cen, and 19p13.11-13.32 (Figures 1B,2B).

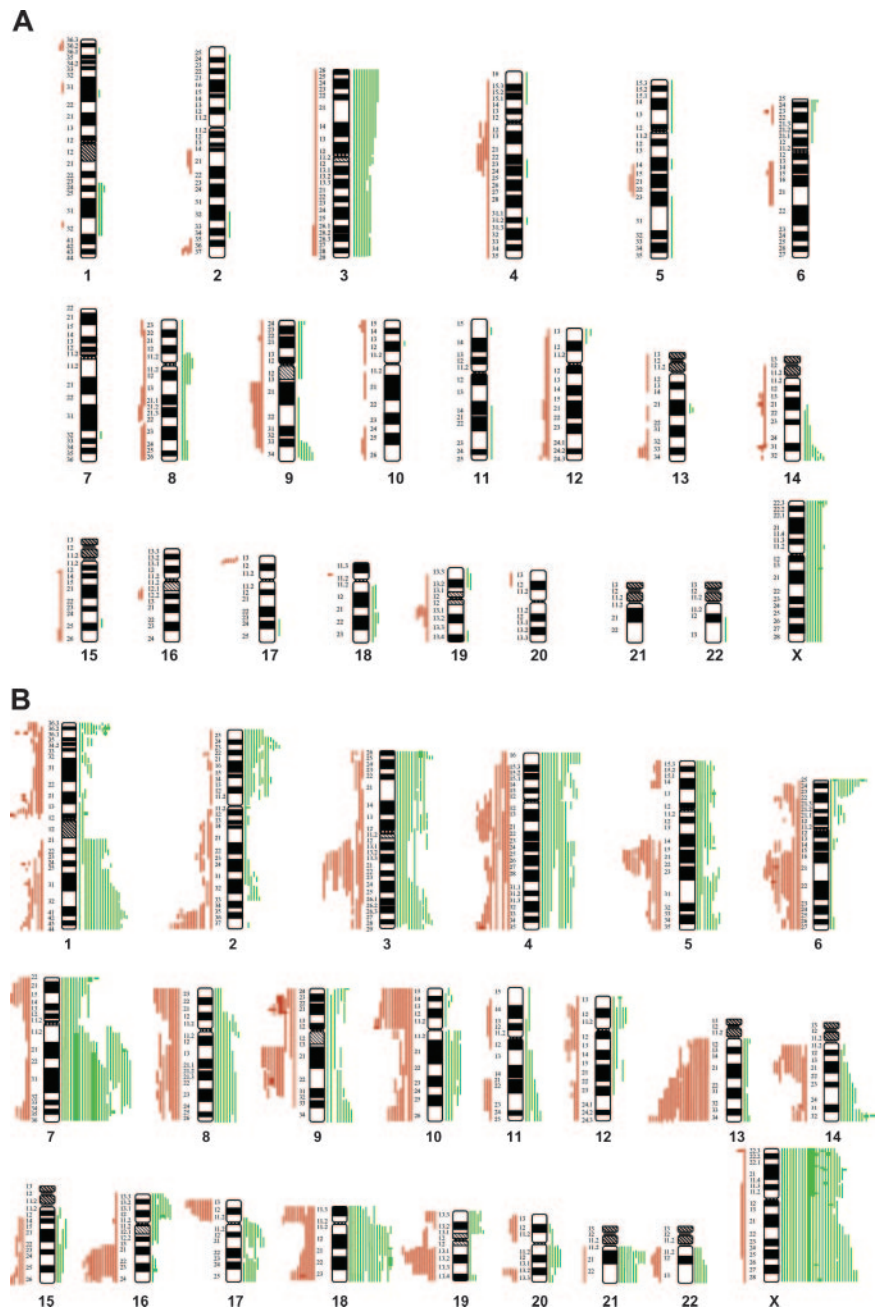
Comparison of genomic profiles of acute and lymphoma types

A comparative analysis of the differences in genomic frequencies between acute and lymphoma types identified several common regions for these 2 subtypes. The common regions of gains were found on 3p36-q12, 3q25-29, 8q24, 9p24, 9q34, and 14q32, and those of losses on 2q37, 4q21, 6q14, 9p21, 9q21, 17p13.1, and 19q13. Statistically significant differences were a gain of 3p26-q26 for the acute type and gains at 1q22-23, 1q41-44, 2p25, 4q21-22, 4q26-27, 7p22, and 7q11-36, and losses of 10p12, 13q21-32, 16q21-22, and 18p11 for the lymphoma type. The regions characteristic of each type as determined are listed in Table 3.

Recurrent genomic amplifications, homozygous losses, and candidate target genes

Recurrent regions (≥ 2 patients) of high-level amplification (\log_2 ratio > +1.0) were found at 1p36, 6p25, 7p22.2, 7q21-q22, 7q31-q36, and 14q32 (Table 4) in the lymphoma-type samples, and

Figure 2. Ideograms of acute and lymphoma types of ATLL. Summary of the chromosomal imbalance detected in 17 acute-type patients (A) and 49 lymphoma-type patients (B). Lines on the left (red) of the ideograms indicate losses, and those on the right (green) indicate gains. Red rectangles on the left represent homozygous losses (\log_2 ratio < -1.0), and green rectangles on the right represent high copy number gains (\log_2 ratio $> +1.0$).



no recurrent amplifications or homozygous losses in the acute type. In an attempt to identify target genes in the high-level amplification regions, those with amplification detected by a single BAC clone were further analyzed (Figure 3). The 3 regions containing candidate genes that have been implicated in lymphoid malignancies were *IRF4* at 6p25.3, *CARMA1* at 7p22.2, and *BCL11B* at 14q32 (2 patients each).¹⁷⁻¹⁹ Candidate target genes of the other regions (eg, 1p36, 7q21-q22, and 7q31-q36) are currently being investigated.

A recurrent region of homozygous loss (\log_2 ratio < -1.0) was found at 9p21.3. As shown in Table 4, the most frequently detected clone of homozygous loss at 9p21.3 was RP11-149I2 (2 cases: D1679 and D1687), which contains the *CDKN2A* and *CDKN2B* tumor suppressor genes. Other recurrent regions of homozygous loss are suspected to be 6q21 and 13q32.

Real-time quantitative PCR analysis for *IRF4*, *CARMA1*, and *BCL11B*

IRF4, *CARMA1*, and *BCL11B* of the 6p25, 7p22, and 14q32 regions were examined for their potential as candidate target genes. These genes are included in the BAC clones with high copy number gains (RP11-498D18, *CARMA1*; and RP11-233K4, *IRF4*) or located very close to such BAC clone (*BCL11B*; 300 kb telomeric to RP11-1127D7). To identify the candidate target genes for these genomic regions, we performed RQ-PCR analysis for 21 patients either with or without this gain/amplification. Although the statistical power of this analysis is limited because of the small number of cases, the expression levels of *CARMA1* of the patients with copy number gains at 7p22 were significantly higher than of those without (Mann-Whitney *U* test, $P = .045$). However, high expression of *CARMA1* was found in the acute type regardless of the 7p22

Table 3. Regions of genomic alterations characteristic of acute or lymphoma types

Chromosome band*	Megabases	Acute type†	Lymphoma type‡
Gain			
1q22-23.1	3	0	11
1q41-44	29.3	0	12-17
2p25	3.1	0	10-13
3p26.3-q26.2	0.2-170.85	6-11‡	4-14
4q21.1-22.1	76.5-92.2	0	10-12
4q26-27	115.7-120.3	0	10-12
7p22.2-22.3	0.5-3.7	0	10-13
7q11.23-7q36.3	76.2-156.9	0-1	15-28
Loss			
10p12.31-12.1	20-28.3	0-1	11-15
13q21.1-q32.1	49.45-91	0-1	10-20
16q21-q22.2	9.6-73.1	0	10-13
18p11.22	8.7-10.1	0	12

For acute-type ATLL, n = 17; for lymphoma-type ATLL, n = 49.

*Regions are listed that showed significant differences in frequency between acute and lymphoma types.

†Number of cases with genomic alterations.

‡Characteristic region of acute type.

gain/amplification. We therefore concluded that the *CARMA1* gene is a target for 7p22 genomic amplification in the lymphoma type but not in the acute type. Repeated experiments showed similar results with a variance of less than 5%; representative data are shown in Figure 4.

With regard to the 14q32 region, RQ-PCR for *BCL11B* failed to demonstrate high-level expression in the cases with high copy number gains, indicating that *BCL11B* is not a candidate gene for the 14q32 region of the lymphoma type (Figure 5). Interestingly, high-level expression of *BCL11B* was noted in the acute type lacking genomic amplification. Various levels of *IRF4* expression were observed regardless of genomic gains, indicating that *IRF4* is not a likely candidate gene of this region (data not shown).

Discussion

ATLL is categorized as a single-disease entity; the neoplasm originated from HTLV-I-infected T cells in the World Health Organization (WHO) classification, although the disease is comprised of 4 subtypes—smoldering, chronic, lymphoma, and acute—which reveal distinct clinicopathologic features.⁷

Previous cytogenetic analysis of ATLL indicated that this disease is characterized by complicated and miscellaneous genomic alterations. Kamada et al studied 107 patients with ATLL and reported recurrent cytogenetic abnormalities, including gains of chromosomes 3, 7, and 21, and various losses.⁸ Tsukasaki et al analyzed 46 patients with aggressive ATLL (acute and lymphoma types) by means of chromosomal CGH and reported frequent genomic gains at 3p, 7q, and 14q, and losses at 6q and 13q.¹⁰ They also demonstrated that aggressive ATLL featured significantly more frequent genomic aberrations than did indolent types such as

Table 4. List of BAC/PAC clones showing recurrent high copy number gains and homozygous losses in lymphoma type

Clone name*	Cytogenetic position	Gain/loss, no. patients†	Amplification/homozygous loss, no. patients‡	Gene§
Gain				
RP3-510D11	1p36.22	12	2	<i>H6PD, LOC440558</i>
RP5-888M10	1p36.21	11	2	<i>VPS13D</i>
RP5-1177E19	1p36.21	9	2	<i>PRDM2</i>
RP11-233K4	6p25.3	18	2	<i>IRF4</i> ¶
RP11-498D18	7p22.2	12	2	<i>CARMA1</i> , <i>GNA12</i>
RP5-911H5	7q21.2	22	2	<i>ANKIB1</i>
RP11-736C20	7q21.2	23	2	<i>CALCR</i>
RP11-148A10	7q22.2	26	2	<i>LHFPL3</i>
RP11-77E2	7q22.3	25	2	<i>DLG, LAMB1, LAMB4</i>
RP11-573B16	7q31.1	25	2	—
RP11-9C22	7q31.33	25	2	<i>SNF1</i>
RP11-66F23	7q31.33	24	2	<i>NYD-SP18, CALU, OPN1SW, DKFZP434G156, FLNC, ATP6V1F, LOC375616</i>
RP11-35B6	7q31.33	24	2	<i>KIAA0828, FAM40B</i>
RP11-233L24	7q33	21	2	—
RP4-659J6	7q33	24	2	<i>ZC3HDC1, KIAA1718</i>
RP11-188A12	7q33	20	2	—
RP11-796I2	7q35	17	2	<i>PRKAG2, LOC441301, GALNTL5</i>
RP11-476H24	7q36.2	18	2	<i>DPP6</i>
RP11-691F21	7q36.3	18	2	<i>LOC285889</i>
RP11-452C13	7q36.3	16	2	<i>PTPRN2</i>
RP11-1127D7	14q32.2	21	2	<i>FLJ25773</i> ,¶ <i>RPL3P4</i> ,¶ <i>BCL11B</i> ¶¶
Loss				
RP1-101M23	6q21	12	2	<i>PRDM1</i>
RP11-149I2	9p21.3	14	2	<i>MTAP, CDKN2A</i> , <i>CDKN2B</i> , <i>NSGX</i>
RP11-214L15	9p21.3	7	2	—
RP11-468C2	9p21.3	5	2	—
RP11-461N23	13q32.1	24	2	<i>GPR18, PHGDHL1, EBI2</i>

*List of BAC clones from p telomere to q telomere are listed for each chromosome number.

†Gain was defined as log₂ ratio +0.2 to +1.0, loss as log₂ ratio -1.0 to -0.2.

‡Amplification was defined as log₂ ratio greater than +1.0 and homozygous loss as log₂ ratio less than -1.0.

§All of the genes located on the BAC/PAC clones. If there were any oncogenes in the clone adjacent to the amplified or lost one, they were listed.

¶The names of genes located in the BAC clones adjacent to RP11-1127D7 are listed. BCL11B is 0.3 Mb telomeric to RP11-1127D7.

¶¶These genes have been implicated in lymphoid malignancies.¹⁷⁻²¹

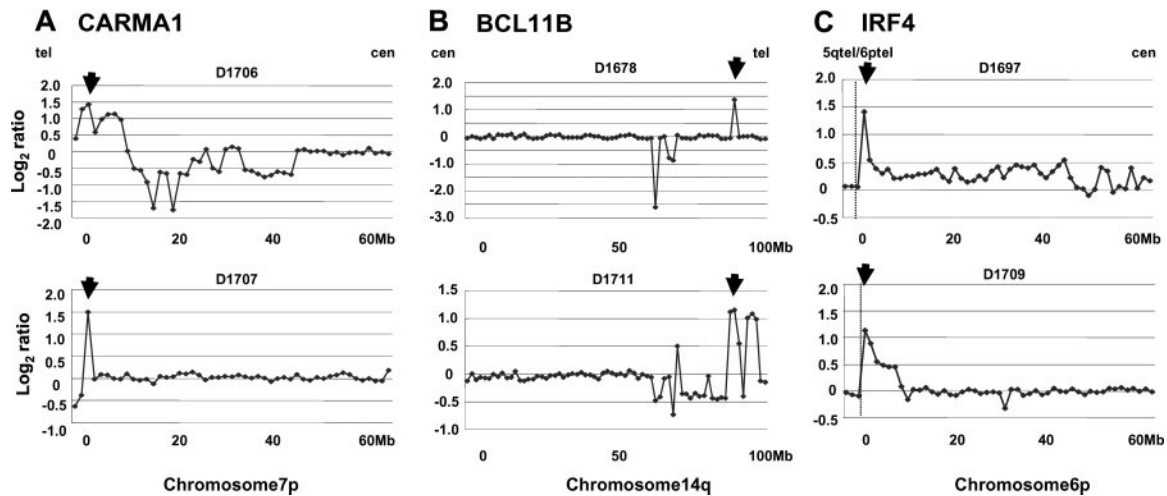


Figure 3. Individual genome profiles of amplification at 6p, 7p, and 14q. Although there were only 2 lymphoma-type cases with high copy number gains, 3 regions are shown because they contained genes implicated in lymphomagenesis. No high copy number gains were found in acute-type cases. (A) Individual genome profiles of high copy number gains at 7p22.2 for 2 patients (D1706 and D1707). Horizontal lines indicate the megabase (Mb) from the 7p telomere to the centromere, and vertical lines show the log₂ ratio. Spots are ordered contiguously from the p telomere to the centromere, with an average resolution of 1.3 Mb. The threshold for gain and loss was defined as a log₂ ratio of +0.2 and -0.2, respectively. The arrow above each graph represents the highest peak at 7p22.2. RP11-498D18 located in the peak contains *CARMA1*. (B) Individual genome profiles of high copy number gains at 14q32 for 2 patients (D1678 and D1711). Spots are ordered contiguously from the 14q centromere to the 14q telomere. The arrow above each graph represents the highest peak at 14q32. RP11-1127D7 located in the peak is 0.3 Mb telomeric to *BCL11B*. (C) Individual genome profiles of high copy number gains at 6p25 for 2 patients (D1697 and D1709). Spots are ordered contiguously from the 6p telomere to the 6p centromere. The arrow above each graph represents the highest peak at 6p25. RP11-233K4 located in the peak contains *IRF4*. Based on information from the Ensembl Genome Data Resources of the Sanger Center Institute and NCBI. Vertical dotted lines represent the boundary between 5q and 6q telomeres.

chronic and smoldering. However, they did not perform a comparative analysis of genomic alterations in acute and lymphoma types. Our study showed that gain at chromosome 3p26-q26 was a frequent genomic aberration of the acute type, while gain at 7q and loss at 13q were characteristic of the lymphoma type.

The common genomic alterations may represent the common oncogenic changes for both types, while differences in their genome profiles may represent different clinical phenotypes. The loss of 9p21 was detected in 20% of patients with acute ATLL and

33% of patients with lymphoma ATLL. The loss of 9p21, which harbors the *CDKN2A* and *CDKN2B* tumor suppressor gene, has been frequently found in aggressive ATLL but not infrequently in indolent types.^{20,21} This suggests that deregulation of tumor suppressor genes such as *CDKN2A* and *CDKN2B* is likely to lead to the transition from indolent to aggressive type. Gain of the 3p26-q26 region is characteristic of the acute type of ATLL, which in turn is characterized by a leukemic phase with flower cells. Recently, it has been demonstrated that phosphatidylinositol 3-kinase, catalytic, beta (*PIK3CB2*) located at 3q22.3 is associated with flower cell formation and the cellular proliferation of ATLL.²² It is tempting to speculate that the gain of 3p26-q26 results in aberrant

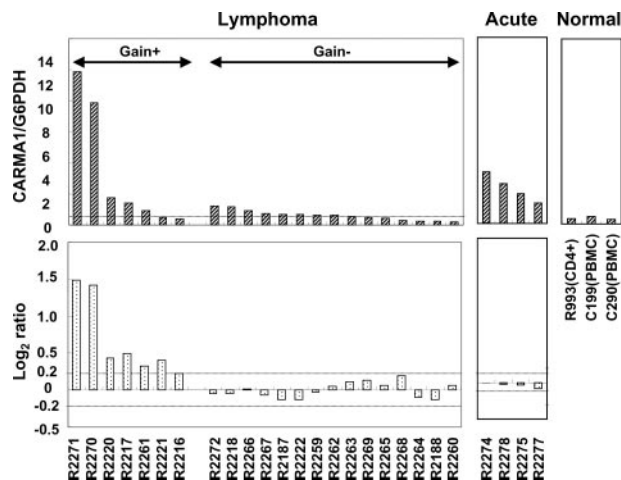


Figure 4. RQ-PCR for *CARMA1* and correlation of genomic amplification. RQ-PCR was used to detect the expression level of *CARMA1* in ATLL patients with or without 7p22 gain/amplification. Twenty lymphoma-type cases were divided into 2 groups, 1 group with copy number gain/amplification (gain +) and the other group without any copy number change (gain -). The top panels show expression levels of *CARMA1* determined by RQ-PCR, while the bottom panels indicate genomic profiles determined by array CGH. The horizontal dotted line in the gain group indicates the mean value (0.603) of the expression level (SD, 0.312). Four patients with acute-type ATLL are represented in the center panels. For comparison, 1 sample of CD4⁺ T cells isolated from peripheral blood mononuclear cells (PBMCs) and 2 samples of PBMCs were examined by RQ-PCR (right panels).

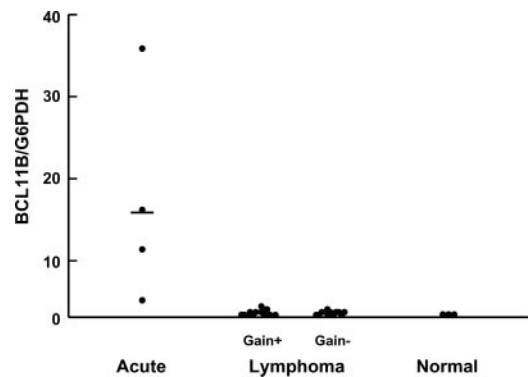


Figure 5. RQ-PCR for *BCL11B* in acute and lymphoma types. RQ-PCR was used to detect expression levels of *BCL11B* in acute and lymphoma types of ATLL. Four patients with acute-type ATLL showed high levels of *BCL11B* expression, although none of them showed any genomic change at RP11-1127D7. The horizontal bar indicates the mean expression level (16.32). Eleven patients with lymphoma-type ATLL with gains at RP11-1127D7 and 10 patients without any genomic change are also shown. None of these patients showed any significant level of expression. For comparison, *BCL11B* expression was examined in 1 CD4⁺ PBMC sample and 2 PBMC samples (Normal). The 4 acute-type patients showed significantly higher expression than did the 21 lymphoma-type patients. (Acute type versus lymphoma type with 14q32 gain [+]: Mann-Whitney *U* test, *P* = .002; acute type versus lymphoma gain [-]: Mann-Whitney *U* test, *P* = .005).

overexpression of the *PI3-kinase*, which then leads to the characteristic clinicopathologic features of the acute type. The most frequent gain characteristic of the lymphoma type is gain of 7q11-36.3 (57%), which was absent from the acute type. The most frequent loss characteristic of the lymphoma type is that of 13q21.1-q32.1 (41%), which was found in only 1 (6%) of 17 patients with the acute type. The candidate genes for these regions, as well as several other regions of lymphoma type which showed significant alterations, may well be responsible for the characteristic clinicopathologic features of the lymphoma type.

The comparative analysis of the genome profiles of acute and lymphoma types identified distinct patterns of genomic alteration, suggesting that these entities might use distinct genomic pathways to develop tumors. The acute type of ATLL may develop tumors via a different mechanism such as translocation or/and mutation with fewer genomic alterations, whereas the lymphoma type may do so through a stepwise process with accumulation of genetic alterations.

We were able to demonstrate that *CARMA1* is a possible target of 7p22 amplification in the lymphoma type, making this the first report of aberrant *CARMA1* expression in human cancer. *CARMA1* is a lymphocyte-specific member of the membrane-associated guanylate kinase (MAGUK) family of scaffolding proteins. It interacts with BCL10 via its caspase-recruitment domain (CARD), functions as an intermediate in the T-cell receptor (TCR) signal transduction pathway²³⁻²⁵ and is a critical regulator of TCR inducing nuclear factor- κ B (NF- κ B) activation. Because NF- κ B is known to be constitutively activated in primary adult T-cell leukemia cells, its activation may be essential for ATLL development.²⁶

Overexpression of *CARMA1* leading to activation of the NF- κ B pathway might play a crucial role in the tumorigenesis of acute and lymphoma types. In the lymphoma type, overexpression of *CARMA1* was found in patients with 7p22 amplification, while in the acute type, *CARMA1* was overexpressed without any 7p22 genomic gain. This makes it likely that a still unknown mechanism other than genomic amplification is responsible for *CARMA1* activation in the acute type.

It is known that the viral protein Tax induces the activation and nuclear translocation of NF- κ B,²⁷⁻³⁰ but primary ATLL cells express only a low level of Tax mRNA and protein.^{31,32} These facts indicate that there must be a mechanism other than Tax for NF- κ B activation. *CARMA1* overexpression detected in our study is one

of the mechanisms leading to constitutive activation of NF- κ B in ATLL cells regardless of the level of Tax. However, the presence of patients with lymphoma-type ATLL lacking *CARMA1* overexpression indicates that other pathways for NF- κ B activation may exist in ATLL.

RQ-PCR examination of *BCL11B* gene³³ expression for acute and lymphoma types showed that genomic amplifications of 14q32 did not correlate well with the expression levels of this gene. This means that *BCL11B* gene is not a target for 14q32 genomic amplification. Interestingly, however, considerably higher levels of *BCL11B* expression irrespective of 14q32 amplification were found in the acute type, suggesting that a mechanism other than genomic amplification induces *BCL11B* overexpression. Since several studies have shown that inv(14)(q11;q32) and t(14;14)(q11;q32) are recurrent chromosomal aberrations in ATLL,^{34,35} aberrant overexpression of *BCL11B* may be due to translocation of 14q.¹⁸ A candidate gene other than *BCL11B* must therefore exist in this 14q32 region of amplification for the lymphoma type and warrants further investigation. The difference in the expression profile of *BCL11B* between acute and lymphoma types also supports the concept that acute and lymphoma types are different disease entities.

In conclusion, genome profiling by array CGH demonstrated that the lymphoma type is characterized by more frequent gains and losses than is the acute type, and it was found that the patterns of genome profiles are also different for these 2 types. *CARMA1* was identified as a possible target of 7p22 amplification in the lymphoma type but no such amplification was found in the acute type although the expression of 7p22 was high. *BCL11B* was not overexpressed in the lymphoma type with 14q32 amplification but a relatively high expression of *BCL11B* was found in the acute type regardless of 14q32 amplification. These results suggest that acute and lymphoma types are distinct subtypes, and may develop via distinct genomic/genetic pathways.

Acknowledgments

The outstanding technical assistance of Ms H. Suzuki and Ms Y. Kasugai is very much appreciated. We also wish to thank Dr Ryuzo Ohno, the chancellor of Aichi Cancer Center, for his overall support.

References

- Uchiyama T, Yodoi J, Sagawa K, Takatsuki K, Uchino H. Adult T-cell leukemia: clinical and hematologic features of 16 cases. *Blood*. 1977;50:481-492.
- Poiesz BJ, Ruscetti FW, Gazdar AF, et al. Detection and isolation of type C retrovirus particles from fresh and cultured lymphocytes of a patient with cutaneous T-cell lymphoma. *Proc Natl Acad Sci U S A*. 1980;77:7415-7419.
- Yoshida M, Seiki M, Yamaguchi K, Takatsuki K. Monoclonal integration of human T-cell leukemia provirus in all primary tumors of adult T-cell leukemia suggests causative role of human T-cell leukemia virus in the disease. *Proc Natl Acad Sci U S A*. 1984;81:2534-2537.
- Tajima K, Kamura S, Ito S, et al. Epidemiological features of HTLV-I carriers and incidence of ATL in an ATL-endemic island: a report of the community-based co-operative study in Tsushima, Japan. *Int J Cancer*. 1987;40:741-746.
- Okamoto T, Ohno Y, Tsugane S, et al. Multi-step carcinogenesis model for adult T-cell leukemia. *Jpn J Cancer Res*. 1989;80:191-195.
- Shimoyama M. Diagnostic criteria and classification of clinical subtypes of adult T-cell leukaemia-lymphoma: a report from the Lymphoma Study Group (1984-87). *Br J Haematol*. 1991;79:428-437.
- Kikuchi M, Jaffe ES, Raffkiaer E. Adult T-cell leukemia/lymphoma. In: Jaffe ES, Harris NL, Stein H, Vardiman JW, eds. *World Health Classification of Tumors: Pathology & Genetics of Tumours of Haematopoietic and Lymphoid Tissues*. IARC press, Lyon; 2001:200-203.
- Kamada N, Sakurai M, Miyamoto K, et al. Chromosome abnormalities in adult T-cell leukemia/lymphoma: a karyotype review committee report. *Cancer Res*. 1992;52:1481-1493.
- Itoyama T, Chaganti RS, Yamada Y, et al. Cytogenetic analysis and clinical significance in adult T-cell leukemia/lymphoma: a study of 50 cases from the human T-cell leukemia virus type-1 endemic area, Nagasaki. *Blood*. 2001;97:3612-3620.
- Tsukasaki K, Krebs J, Nagai K, et al. Comparative genomic hybridization analysis in adult T-cell leukemia/lymphoma: correlation with clinical course. *Blood*. 2001;97:3875-3881.
- Ohshima K, Kikuchi M, Yoshida T, Masuda Y, Kimura N. Lymph nodes in incipient adult T-cell leukemia-lymphoma with Hodgkin's disease-like histologic features. *Cancer*. 1991;67:1622-1628.
- Ota A, Tagawa H, Kaman S, et al. Identification and characterization of a novel gene, *C13orf25*, as a target for 13q31-q32 amplification in malignant lymphoma. *Cancer Res*. 2004;64:3087-3095.
- Tagawa H, Tsuzuki S, Suzuki R, et al. Genome-wide array-based comparative genomic hybridization of diffuse large B-cell lymphoma: comparison between CD5-Positive and CD5-negative cases. *Cancer Res*. 2004;64:5948-5955.
- Tagawa H, Kaman S, Suzuki R, et al. Genome-wide array-based CGH for mantle cell lymphoma: identification of homozygous deletions of the proapoptotic gene *BIM*. *Oncogene*. 2005;24:1348-1358.
- Suguro-Katayama M, Suzuki R, Kasugai Y, et al. Heterogeneous copy numbers of API2-MALT1

- chimeric transcripts in mucosa-associated lymphoid tissue lymphoma. *Leukemia*. 2003;17:2508-2512.
16. Wright SP. Adjusted P-values for simultaneous inference. *Biometrics*. 1992;48:1005-1013.
 17. Sharma S, Grandvaux N, Mamane Y, et al. Regulation of IFN regulatory factor 4 expression in human T cell leukemia virus-I-transformed T cells. *J Immunol*. 2002;169:3120-3130.
 18. Gesk S, Martin-Subero JI, Harder L, et al. Molecular cytogenetic detection of chromosomal breakpoints in T-cell receptor gene loci. *Leukemia*. 2003;17:738-745.
 19. Egawa T, Albrecht B, Favier B, et al. Requirement for CARMA1 in antigen receptor-induced NF-kappa B activation and lymphocyte proliferation. *Curr Biol*. 2003;13:1252-1258.
 20. Hatta Y, Hiramata T, Miller CW, et al. Homozygous deletions of the p15 (MTS2) and p16 (CDKN2/MTS1) genes in adult T-cell leukemia. *Blood*. 1995;85:2699-2704.
 21. Yamada Y, Hatta Y, Murata K, et al. Deletions of p15 and/or p16 genes as a poor-prognosis factor in adult T-cell leukemia. *J Clin Oncol*. 1997;15:1778-1785.
 22. Fukuda R, Hayashi A, Utsunomiya A, et al. Alteration of phosphatidylinositol 3-kinase cascade in the multilobulated nuclear formation of adult T cell leukemia/lymphoma (ATLL). *Proc Natl Acad Sci U S A*. 2005;102:15213-15218.
 23. Wang D, You Y, Case SM, et al. A requirement for CARMA1 in TCR-induced NF-kappa B activation. *Nat Immunol*. 2002;3:830-835.
 24. Gaide O, Favier B, Legler DF, et al. CARMA1 is a critical lipid raft-associated regulator of TCR-induced NF-kappa B activation. *Nat Immunol*. 2002;3:836-843.
 25. Pomerantz JL, Denny EM, Baltimore D. CARD11 mediates factor-specific activation of NF-kappaB by the T cell receptor complex. *EMBO J*. 2002;21:5184-5194.
 26. Mori N, Fujii M, Ikeda S, et al. Constitutive activation of NF-kappaB in primary adult T-cell leukemia cells. *Blood*. 1999;93:2360-2368.
 27. Kanno T, Brown K, Franzoso G, Siebenlist U. Kinetic analysis of human T-cell leukemia virus type I Tax-mediated activation of NF-kappa B. *Mol Cell Biol*. 1994;14:6443-6451.
 28. Sun SC, Elwood J, Beraud C, Greene WC. Human T-cell leukemia virus type I Tax activation of NF-kappa B/Rel involves phosphorylation and degradation of I kappa B alpha and RelA (p65)-mediated induction of the c-rel gene. *Mol Cell Biol*. 1994;14:7377-7384.
 29. Lacoste J, Petropoulos L, Pepin N, Hiscott J. Constitutive phosphorylation and turnover of I kappa B alpha in human T-cell leukemia virus type I-infected and Tax-expressing T cells. *J Virol*. 1995;69:564-569.
 30. Suzuki T, Hirai H, Murakami T, Yoshida M. Tax protein of HTLV-1 destabilizes the complexes of NF-kappa B and I kappa B-alpha and induces nuclear translocation of NF-kappa B for transcriptional activation. *Oncogene*. 1995;10:1199-1207.
 31. Kinoshita T, Shimoyama M, Tobinai K, et al. Detection of mRNA for the tax1/rex1 gene of human T-cell leukemia virus type I in fresh peripheral blood mononuclear cells of adult T-cell leukemia patients and viral carriers by using the polymerase chain reaction. *Proc Natl Acad Sci U S A*. 1989;86:5620-5624.
 32. Furukawa Y, Osame M, Kubota R, Tara M, Yoshida M. Human T-cell leukemia virus type-1 (HTLV-1) Tax is expressed at the same level in infected cells of HTLV-1-associated myelopathy or tropical spastic paraparesis patients as in asymptomatic carriers but at a lower level in adult T-cell leukemia cells. *Blood*. 1995;85:1865-1870.
 33. Satterwhite E, Sonoki T, Willis TG, et al. The BCL11 gene family: involvement of BCL11A in lymphoid malignancies. *Blood*. 2001;98:3413-3420.
 34. Sadamori N, Nishino K, Kusano M, et al. Significance of chromosome 14 anomaly at band 14q11 in Japanese patients with adult T-cell leukemia. *Cancer*. 1986;58:2244-2250.
 35. Miyamoto K, Tomita N, Ishii A, et al. Specific abnormalities of chromosome 14 in patients with acute type of adult T-cell leukemia/lymphoma. *Int J Cancer*. 1987;40:461-468.